PEYTO
GLACIER
ONE CENTURY OF SCIENCE

LINKING THE WEATHER TO GLACIER HYDROLOGY AND MASS BALANCE AT PEYTO GLACIER

D. Scott Munro

Department of Geography, University of Toronto at Mississauga, Ontario, L5L 1C6, Canada

ABSTRACT

Attempts have been made to link weather variations at Peyto Glacier to mass balance fluctuations. On the larger scale of inquiry, associations have been found between seasonal components of the mass balance and synoptic weather types. Also, there are significant correlations with temperature and precipitation records from regional weather stations. The smaller scale of study features micro-meteorological investigations to document the energy components of summer ablation and surface meltwater generation.

Field measurements of the energy exchange components in summer show that solar short-wave radiation and atmospheric long-wave radiation supply the glacier surface with approximately 16 and 25 MJ m^{-2} of energy per day respectively, thus constituting important heat sources for the melting of ice and snow. Over snow, the reduction of net long-wave radiation loss by cloud cover may speed up the retreat of the snowline, thus preparing the glacier for high levels of meltwater production later in the season. Turbulent transfer of sensible heat from air to ice is a significant energy source, contributing 3 to 4 MJ m^{-2} to the daily melt. It is strongly controlled by

katabatic wind flow, which is best developed in fair, anticyclonic weather. Latent heat exchange due to turbulent water vapour transfer is only a minor component of the surface energy exchange picture, supplying less than 0.5 MJ m^{-2} to melting. The cooling effect of turbulent heat loss to the glacier may be felt for at least 20 m above the glacier surface.

The conversion of melt energy data into ablation estimates yields reasonably accurate results for ice, where values range from -1 to 8 mm h^{-1} of water equivalent ice melt. Negative estimates, and a tendency to overestimate ablation at the higher end of the range, are signs of weathering crust development. Less success is achieved over snow because of its variable density structure. The energy balance approach works sufficiently well over glacier ice and snow to constitute the basis of a modelling scheme for both the ablation phase and the accumulation phase of the mass balance cycle. Surface energy exchange, acting in consort with the precipitation regime, is thus seen to be the essential link between weather variations and mass balance fluctuations.

INTRODUCTION

The decision to begin mass balance measurements at Peyto Glacier brought with it attempts to monitor daily weather in the basin. Most data yielded by this effort comprise a mixture of hygrothermograph and precipitation records, supplemented in the early years by observer readings of sunshine hours, total solar radiation, wind and sky conditions. The need for observers restricted data collection to the summer melt period in those years, thus leaving the winter period unknown, except for what could be surmised from the winter mass balance records and climatic data for Banff, Lake Louise and Jasper.

Summer research activity involved micro-meteorological studies from time to time. They were mainly directed toward gaining a better understanding of the melt response to surface energy exchange (Föhn, 1973; Derikx, 1975; Munro, 1990). Occasionally this included detailed study of the atmospheric boundary layer near the ice, principally with regard to the behaviour of the katabatic wind (Munro and Davies, 1977; Stenning *et al.*, 1985). Illuminating though the results of these efforts are, they stand as case studies which lack the context of the glacier's seasonal climatology, a context which is best understood from a local year-round data base.

The opportunity to obtain such a data base came during the summer of 1987, with the installation of an automatic weather station at Peyto Glacier Base Camp (Figure 1). Initial difficulties with instrumentation, cold weather operation and power supply were overcome, such that hourly measurements of solar radiation, air temperature, atmospheric humidity, windspeed and precipitation are now recorded throughout the year. The daily means and totals that can be constructed from the data are interesting in themselves. But the key question is how best to apply the data to resolving the problem of linking the glacier mass balance fluctuations, and associated hydrological response, to the stimulus of the weather.

Figure 1. *Peyto Glacier weather station, showing sensor locations for air temperature, solar radiation and shielded precipitation gauge.*

One may ponder the question in relation to seasonal patterns of solar radiation, air temperature and precipitation, the principal climatic determinants of the mass balance cycle (Figure 2). In a regime such as this, where substantial amounts of precipitation can occur throughout the year, it is readily appreciated that snow is expected to accumulate in the sub-freezing temperatures and weak sunlight of winter, then ablate in the warmth and intense solar radiation of summer. The roles of precipitation as mass supplier and solar radiation as melt energy source are clear in this context, but that of temperature is more complex. The potential for air temperature above freezing to be an important energy supplier is well recognized in the temperature index approach to snow melt estimation (Male and Gray, 1981), its strong association with ablation (Braithwaite and Olesen, 1990a) and its importance to the climate at the glacier equilibrium line (Ohmura *et al.*, 1992). But, its most significant function may be to act as a climatological switch that activates rain and melt events throughout the year.

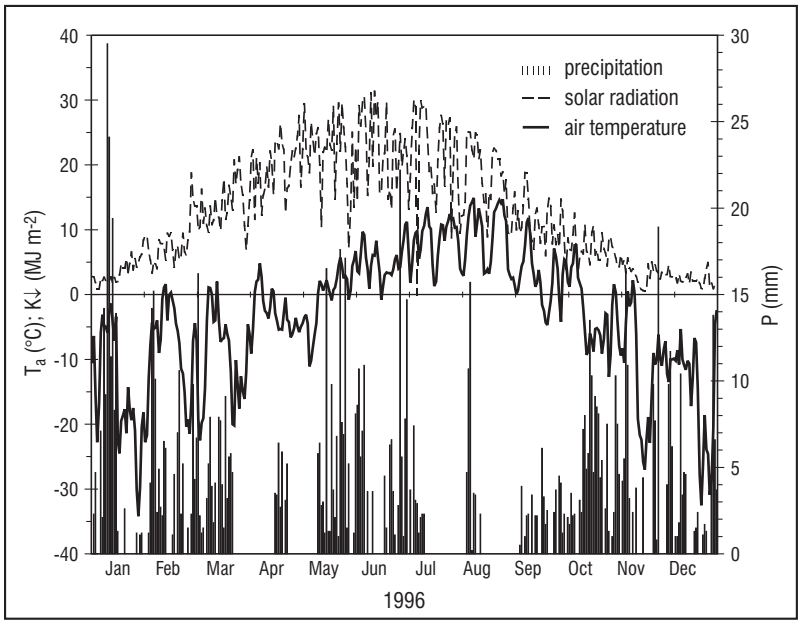

Figure 2. *Day-to-day variations in mean air temperature, T_a, total solar radiation, K↓, and total precipitation, P, at Peyto Glacier weather station.*

REGIONAL CLIMATE AND MASS BALANCE FLUCTUATIONS

The effects of regional climate variation seem to be evident from knowledge that the elevation of the glacier equilibrium line tends to rise through the mountains, from the Pacific Coast to the eastern ranges of the Rocky Mountains, a feature which Østrem (1966, 1973) attributed to a reduction of precipitation as the climatic regimen changes from maritime to continental. This feature has also been documented more widely for North American glaciers (Meier, *et al.*, 1971), where there is an altitudinal rise in the glacier equilibrium line southward through the Western Cordillera, a response to increasing temperature and dryness, as well an eastward rise to the continental interior, a response to decreasing precipitation. If one accepts that such variations in glacier elevation reflect contrasting regional climatologies, then it is natural to ask whether glacier responses to climate change over time might also vary across the mountains.

In the first instance one must establish the nature of the link between weather variations and glacier mass balance fluctuations; that is to say the responses of accumulation and ablation to deviations from climatic norms. Approaches to doing so depend upon the information available. Before the advent of the automatic weather station, there were three principal data sources: synoptic weather charts, year round climate records from Banff, Lake Louise and Jasper, and summer observations at base camp. Also, there were data collected for studies into specific micro-meteorological phenomena, such as boundary layer development in katabatic winds (Munro and Davies, 1977) or the effect of a debris layer on ablation (Nakawo and Young, 1981), where the results obtained are typical of fine summer weather.

Synoptic analysis of glacier response has been applied at the continental scale by Walters and Meier (1989) to examine glacier mass balance variations in western North America. They found that years of positive glacier mass balance in Alaska tended to coincide with negative mass balance years in Alberta, Southern British Columbia and Washington State due to the steering effect of the Aleutian low upon snow bearing weather systems. This effect can be especially strong during the E1 Niño phase of the Southern Oscillation, when a system of ridges and troughs known as the Pacific North America circulation pattern sets in, thus blocking the zonal flow of moist air along the Canada - United States border. The consequences are most strongly felt during winter, and work by Demuth and Keller (2006) illustrates the importance of such synoptic-scale influences on the mass balance fluctuations at Peyto Glacier.

The use of synoptic data to investigate glacier mass balance responses to weather variations in south-western Canada is first exemplified by the work of Yarnal (1984), in which synoptic analysis was applied to Peyto Glacier (Table 1), as well as to Sentinel Glacier (southern Coast Mountains). Winter mass balance data defined the criterion for glacier accumulation response, while Banff maximum temperature data were used as a surrogate for the ablation response. Synoptic weather types were identified in terms of the sea level pressure field at two scales of analysis. One of these, involving a grid spacing of 350 km, was directed toward capturing the regional scale of synoptic variability. The other, with a grid spacing of 700 km, was aimed at the zonal synoptic scale of weather variability in the westerly wind system.

***Table 1**. Synoptic climate and seasonal mass balance response for Peyto Glacier (after Yarnal, 1984).*

SCALE	SEASON	MAIN SYNOPTIC STIMULUS	RESPONSE CRITERION	EXPLAINED VARIANCE
regional	winter	cooler/warmer than normal	less/more accumulation	0.751
	summer	more precipitation per event	less ablation	0.277
zonal	winter	anticyclonic/cyclonic	less/more accumulation	0.870
	summer	cooler than normal	less ablation	0.293

Yarnal's analysis proved to be much better at explaining the accumulation phase of the mass balance cycle than was the case for the ablation period. Furthermore, zonal variations in synoptic patterns had more explanatory power than regional variations, particularly so for the winter mass balance. Low levels of explained variance at both scales for the summer mass balance were attributed to the relatively close proximity of Banff to the eastern margin of the mountains, where it could be influenced by shallow continental air flow from the foothills.

The Peyto results were in stark contrast to those for Sentinel Glacier, where the regional scale explained most of the variance in both seasons. Moreover, the relative importance of zonal-scale synoptic explanation for winter and summer variations at Sentinel was almost the reverse of what was indicated for Peyto. Contrasts between findings for the two glaciers must be viewed with caution, however, in light of a recently discovered need to correct for stake self-drilling and its effects on the Sentinel Glacier mass balance record (Brugman, personal communication). Recent work

indicates that mass balance responses to synoptic conditions at Peyto are to those at Place Glacier, which is also in the southern Coast Mountains (Demuth and Keller, 2006, Figure 12).

A statistical approach to linking weather and mass balance variations at Peyto, Place and Sentinel glaciers was taken by Letréguilly (1988). Changes in equilibrium line altitude, as well as variations in the mass balance records, were examined in relation to temperature and precipitation data collected over the 1966 to 1984 period at climate stations in their respective regions. The mass balance was separated into its summer and winter components which, respectively, were related to different lengths of summer temperature and winter precipitation record. Summer temperature data collected at base camp were included in the analysis for Peyto Glacier, but the strongest correlations were obtained with data collected outside the basin (Table 2).

Table 2. *Strongest correlations between station predictors and Peyto Glacier net, summer and winter mass balance (Letréguilly, 1988). Months (i.e. May-July, inclusive) denote averaging and summation periods.*

PREDICTOR	ANNUAL	SUMMER	WINTER
Average T_{min}	-0.86 (May-July)	0.70 (Jun-Aug)	-----
Average T_{max}	-0.56 (May-July)	0.81 (Jun-Aug)	-----
Total Precipitation	0.51 (Oct-Feb)	-----	0.71 (Oct-Mar)
Station	Jasper	Jasper	Lake Louise

Significant correlations were found using data from Banff, Golden, Calgary and Edmonton as well, but Jasper and Lake Louise correlations tended to be at least 0.1 stronger than the next best station in each category listed in Table 2. Although one should not attach undue importance to a correlation difference of only 0.1, the results are quite plausible, given that Lake Louise is the closest winter precipitation station and that Jasper, despite its greater distance from Peyto than Banff, is possibly more montane. The surprising result to Letréguilly was that summer temperature data from the Peyto station did not produce correlations that were as strong. The only significant summer correlations were with average minimum temperatures taken from June to July, amounting to -0.67 for the net mass balance and 0.60 for the summer balance. Correlations with Jasper data were -0.86 and 0.69, respectively, for the same two months.

When surprising results are obtained it is natural to question the quality of the data. There may, however, be a different explanation. The use of summer temperature data to represent ablation (Yarnal, 1984), or to correlate with it (Letréguilly, 1988), stems from the knowledge that temperature can be an effective melt predictor (Male and Gray, 1981; Braithwaite and Olesen, 1990a). Nevertheless, surface energy exchange studies over glacier ice consistently reveal that, allowing for surface reflectivity, the most powerful melt agent is solar radiation.

So, to the extent that warm conditions are also sunny conditions, good results can be obtained with temperature. The likelihood that temperature correlates well with solar radiation is strong in such cases if the temperature is representative of non-glacierized land cover in the region, where a large variance in the temperature signal is expected. Therefore, poorer results with Peyto station data are quite possibly the consequence of being too close to the glacier, where the local cooling effect of snow and ice must reduce the variance in temperature, thus weakening the explanatory power of the temperature signal.

Cloud cover variability accounts for daily fluctuations within the annual solar radiation pattern (Figure 2). Warm, sunny conditions are expected to produce high ablation rates for exposed glacier ice; cool, overcast conditions low ablation rates. Snow cover, however, can demonstrate the seemingly paradoxical behaviour of ablating most effectively in cool, overcast conditions, provided air temperature remains above the melting point (Ambach, 1974; Wendler, 1986; Serreze and Bradley, 1987). In fact, the change from clear to cloudy conditions over snow can transform a small radiative surplus, due solely to what little net short-wave radiation is absorbed by the highly reflective snow cover, into a greater radiation surplus than before. This is possible because the enhancement of atmospheric long-wave radiation by warm, low level cloud cover can more than compensate for a reduction in net short-wave radiation by the same cloud cover.

A rise in the daily minimum temperature is a natural consequence of the foregoing transformation (Bücker and Dessens, 1991), so it is not surprising to see a strong correlation between reduction in the net mass balance and rise in the average May-July minimum temperature (Table 2). May-July is the period over which snow on the glacier tongue is expected to warm, ripen and disappear. The difference between a positive and a

negative balance year depends not only upon the amount of snow supplied in winter, but also upon how quickly the ice underneath, with its superior ability to absorb solar radiation, can be exposed. The suggestion here is that average minimum temperature during the May-July period is a good indicator of how quickly ice exposure occurs because one expects a considerable difference between the mass balance of a year in which the ice is exposed early in June and one in which the exposure is delayed until the beginning of July.

As demonstrated in the foregoing discussion, synoptic and statistical approaches to investigating glacier responses to climatic change do much to generate ideas about the nature of the relationship. Furthermore, the data bases for such investigations extend over much longer time periods than those which are usually covered by the micro-meteorological approach, periods which are relevant to examining such questions as the impacts of global warming upon glaciers and ice fields (Demuth and Keller, 2006; IAHS(ICSI)/UNEP/UNESCO, 1996, 1999). Nevertheless, micro-meteorology holds the key to understanding how the relationship works, because it is at the heart of the mechanisms that control the gain and loss of surface ice. This is well illustrated by the work of Alt (1987) in the Arctic and by more recent work in the Pyrénées (Hannah and McGregor, 1997), where the emphasis is not so much to connect synoptic types directly to the mass balance data as it is to associate them with characteristic surface energy exchange patterns. Although the importance of energy exchange is most evident during the ablation season, it is active during the accumulation season as well, thus helping to shape the glacier mass balance response throughout the year.

SURFACE ENERGY EXCHANGE

Micro-meteorological studies at Peyto Glacier apply exclusively to the ablation season, as is typical in glaciology, particularly for valley glaciers. This is the preferred season for field work because, not only are working conditions best for measurement equipment, the surface energy balance components generated from the measurements are also the components of surface meltwater generation, M:

$$M = (Q_* + Q_H + Q_E)(\rho_i L_f)^{-1} \qquad (1)$$

in which Q_*, Q_H and Q_E are, respectively, the energy flux densities due to net radiation, sensible heat exchange and latent heat of water vapour transfer between surface and adjacent atmosphere, ρ_i is snow or ice density, and L_f is the latent heat of fusion for ice.

In summer, the energy balance at Peyto (Föhn, 1973; Derikx, 1975; Munro, 1990) is consistent with work done elsewhere during the ablation season (Hay and Fitzharris, 1988; Braithwaite and Olesen, 1990b; van den Broeke, 1997a), wherein most of the melt energy is supplied by Q_*, a substantial amount is obtained from Q_H and only a small amount is due to Q_E . In fact, water vapour transfer at Peyto can often be associated with energy loss because melt season vapour pressure is frequently less than the ice point value of 611 Pa, resulting in evaporation. The energy exchange components are expected to be small during the winter where the need arises to include changes in the heat content of snow and ice as part of the surface energy balance. Such melt as does occur at this time is likely to be refrozen *in situ*.

The Glacier Atmospheric Environment

Observational evidence is confined to the boundary layer of Peyto Glacier (Munro and Davies, 1977), thus leaving one to speculate about the nature of air movement further aloft. Earlier work on Devon Ice Cap by Holmgren (1971), recent work by van den Broeke (1997b) on Pasterze Glacier, Austria, as well as general knowledge about radiative transfer through the atmosphere, are most relevant to assembling a schematic picture which is likely to apply to Peyto Glacier in fair, anticyclonic weather during the ablation season (Figure 3).

The setting is such that one would expect solar short-wave radiation income to increase with altitude due to thinning of the atmosphere and reduced shading from the surrounding topography, while the same factors would cause atmospheric long-wave radiation income to decrease with altitude (Figure 3). A katabatic flow, referred to as the glacier wind, is embedded within a valley wind system which is anabatic by day (Figure 3), katabatic at night. During the day, sensible heat and water vapour carried up glacier from the valley floor by the anabatic wind is entrained into the glacier wind at higher glacier elevations, thus supplying heat for turbulent transfer to the glacier surface. If this scheme is correct, then one would not expect the cooling effect of a valley glacier like Peyto to be felt far beyond its terminus, an expectation which is confirmed by experience.

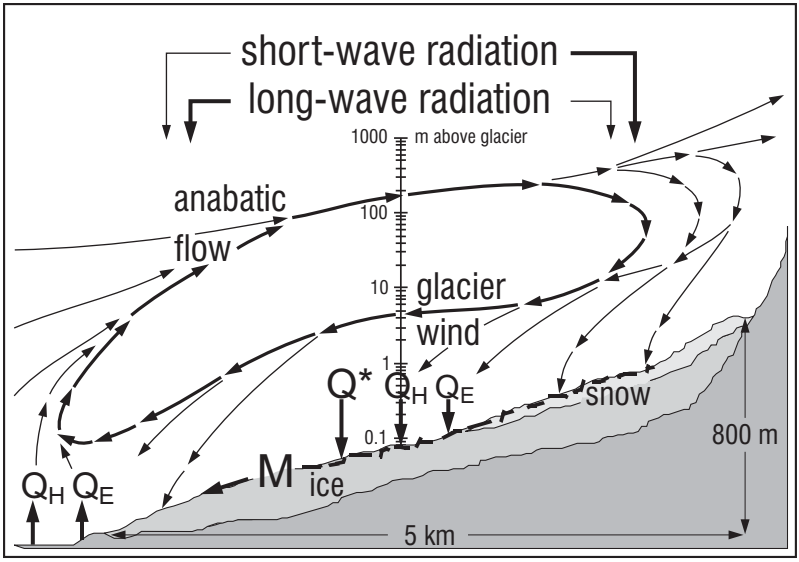

Figure 3. *Glacier air flow and radiation scheme for sunny, anticyclonic weather.*

Previous work at Peyto (Munro and Davies, 1977; Stenning, *et al.*, 1981) indicates the height of maximum glacier wind speed to be in the order of 5 m or more above the glacier surface, a height which seems to agree with similar observations on Pasterze, a glacier which is slightly larger than Peyto (van den Broeke, 1997b). A detailed examination of the profile structure at Peyto (Munro and Davies, 1978) suggests that micro-meteorological theory of the surface boundary layer can be used to calculate turbulent heat exchange, provided the data are collected within 1.5 m of the surface. A thinner boundary layer could apply further up glacier, due to weaker glacier wind development, though this has not been documented.

Measurement and Calculation of Heat Transfer Components

Micro-meteorological technique can be applied to study the details of glacier boundary layer structure (Munro and Davies, 1978; Munro, 1989), but the key to hydrological application is to find robust approaches which will work with minimal data requirements. Melting conditions on glaciers lend themselves particularly well to simplification because the surface is at the ice point of 0°C, 611 Pa, a situation where the bulk transfer approach (Oke, 1987) to turbulent flux calculation can be effective. Consequently, it

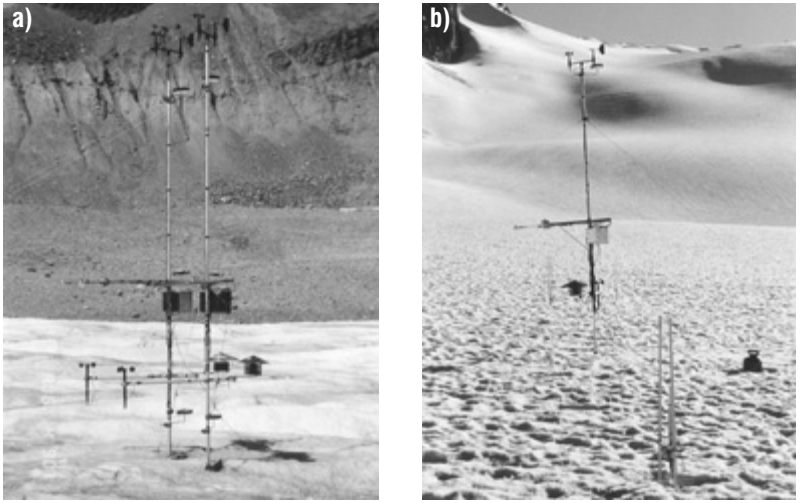

Figure 4. *Instrument arrays for boundary layer and radiation measurements over* ***a)*** *ice on the glacier tongue;* ***b)*** *snow in the upper basin, with ablatometer in foreground. Symbols are defined in the text.*

has been widely used in glacier energy budget studies (Paterson, 1994). This reduces the data requirements for Equation (1) to net radiation, Q_*, air temperature, T, vapour pressure, e, and wind speed, u, at one level above the surface.

Field deployment of suitably robust instrumentation over ice on the glacier tongue is shown in Figure 4a, where an intercomparison of two sensor arrays is being made. Anemometers, with small temperature and humidity shelters, are mounted on masts at 1 m above the ice to maximize the likelihood of measurement within the surface boundary layer. Radiometric sensors point southward, to minimize shadow effects. A 2 m mounting height usually allows downward facing radiometers to receive 95% of their radiation from a viewing area 6 m in radius. Experience has shown that flat rocks, 10 to 15 kg in weight, are effective bases for masts and guy wires. The instrument array effectively 'floats' on the surface, thus maintaining the original sensor mounting heights.

Instrument arrays of this type are lightweight, easily transportable and readily modified to carry additional sensors for radiation or boundary layer work. One sensor array may be left on the glacier tongue, while an

additional array is located above the snowline (Figure 4b), thus allowing concurrent collection of data to use in comparing the energy regimes of the two locations. Although the density of a summer snow pack is approximately half that of ice, the snow surface is sufficiently strong to use the same deployment strategy as that for ice, as well as similar schedules of daily maintenance to keep the masts properly aligned.

It is clear from Figure 4 that ice and snow present contrasting surface conditions for research; it should be kept in mind that they present different topographical settings as well. The high mountain walls adjacent to the glacier tongue reduce the view of the sky, while the higher elevation of the snow site ensures that more of the sky is visible. Therefore, a comparison of results presents an excellent opportunity to test some of the ideas portrayed in Figure 3, beginning with radiative transfer.

Net radiation components

Although net radiation measurement is sufficient in itself for surface energy exchange work, field work at Peyto has usually entailed the measurement of some, or all of its components:

$$Q_* = K\downarrow - K\uparrow + L\downarrow - L\uparrow \qquad (2)$$

in which K and L refer to the short-wave and long-wave radiation components, respectively, the down and up arrows to income and loss. Climatologists refer to incoming short-wave radiation, $K\downarrow$, as global radiation, but it will continue to be referred to here as solar radiation. The incoming long-wave radiation, $L\downarrow$, will simply be referred to as atmospheric radiation. Both $K\downarrow$ and $L\downarrow$ may include small amounts of radiation from the surrounding topography.

Direct measurement of each component in Equation (2) is possible, but the usual approach taken is to measure some of the components directly and to obtain others by residual. For example, the work described here is based upon net radiometer measurements of Q^* and pyranometer measurements of $K\downarrow$ and $K\uparrow$ (Figure 4), where sensor terminology is more fully described in Oke (1987). The residual of the two pyranometric measurements is the net short-wave radiation, $K^* = K\downarrow - K\uparrow$, while the ratio, $\alpha = K\uparrow / K\downarrow$, defines the surface short-wave reflectivity. Given Q^* and K^* it is straightforward to calculate the net long-wave radiation, $L^* = Q^* - K^*$, thus obtaining another residual estimate.

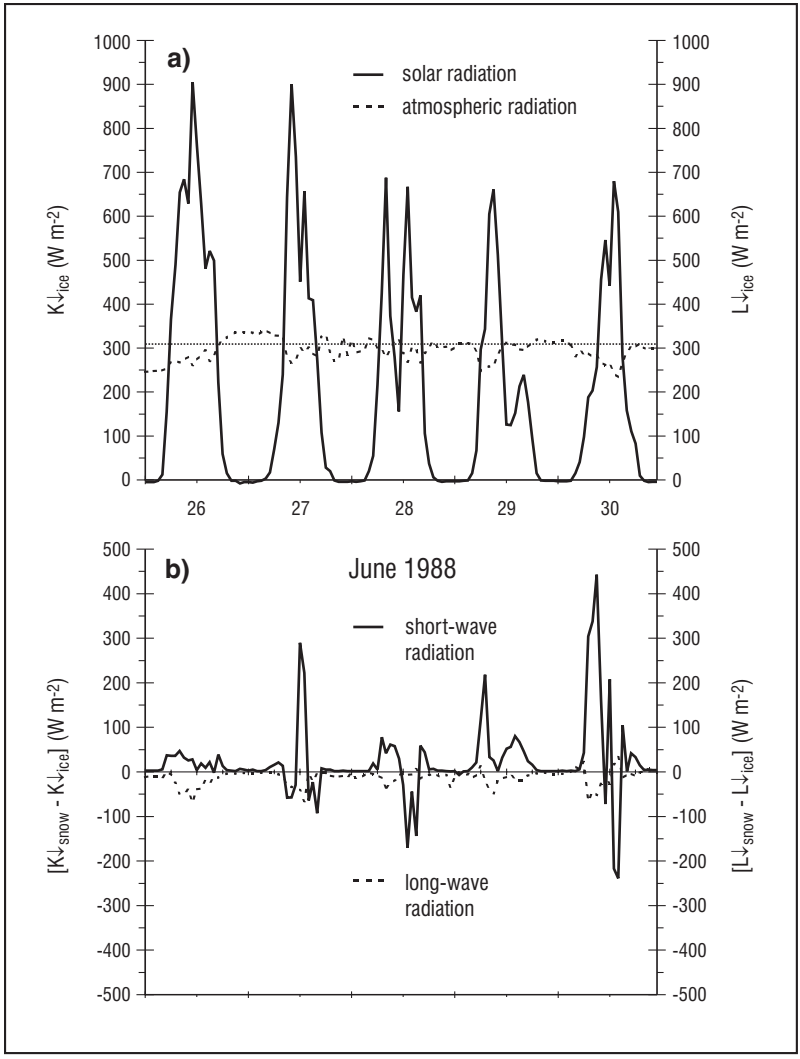

Figure 5. *Peyto Glacier* ***a)*** *incoming radiation amounts to ice surface, with 309 W·m^{-2} reference line;* ***b)*** *differences between radiation incomes of snow and ice.*

Measurements of the long-wave radiation components are more difficult to obtain; none are reported here. But, one may take advantage of the fact that the surface temperature, T_s, of melting snow and ice can be set at the ice point temperature of 273.16°K. Then the Stefan-Boltzmann law may be used to calculate $L\uparrow = \varepsilon_s \sigma T_s^4$ where σ is the Stefan-Boltzmann constant, and the surface emissivity, ε_s, is set to 0.98, the upper end of the documented range for snow and ice (Oke, 1987). The setting of ε_s to the upper end of its range seems to be appropriate in view of the high water content and roughness of the glacier surface during the ablation season. This yields a fixed estimate of 309 $W \cdot m^{-2}$ for $L\uparrow$ which is then used to estimate atmospheric radiation as the residual, $L\downarrow = L^* + L\uparrow$.

The picture which emerges from the data is the classic diurnal pattern (Oke, 1987) in which $K\downarrow$ is characterized by zero to maximum radiation supply, while $L\downarrow$ is a substantial radiation supplier throughout the day (Figure 5a). It can be seen during the daylight hours that the impact of cloud cover is greatest for solar radiation, where substantial reductions in $K\downarrow$ are matched by small increases in $L\downarrow$. As small as cloud induced increases to atmospheric radiation can be, they may occasionally be sufficient to raise $L\downarrow$ above the ice point limit of $L\downarrow$ = 309 W·m-2 , a situation which seems to occur on the night of June 26 (Figure 5a). Thus, although the picture presented here must imply $K_* \geq 0$, it does not necessarily imply $L_* < 0$. There are occasions to consider $L_* \geq 0$ or, at the very least, extremely small values for net long-wave radiation loss.

Caution may be advised in accepting the $L\downarrow$ values as they stand because most radiometers are precise to no better than 5%, so estimation by residual is inherently imprecise, particularly in view of the number of steps taken to obtain $L\downarrow$. Nevertheless, differences between residual $L\downarrow$ values over ice, at an elevation of 2240 m, and snow, at 2510 m, are consistent with expectations. Incoming long-wave radiation at the snow site, where there is more exposure to the sky, tends to be noticeably less than at the ice site, which usually results in $(L\downarrow_{snow} - L\downarrow_{ice}) < 0$ (Figure 5b). Differences between the two are extremely small under cloud cover, but the differences appear to increase on sunny days, when heating of the surrounding topography may enhance the supply of long-wave radiation to the glacier tongue more than it can to the upper basin of the glacier.

Solar radiation differences between ice and snow sites are calculated directly from pyranometric measurements (Figure 5b). They indicate a tendency for $(K\downarrow_{snow} - K\downarrow_{ice}) > 0$, as expected, though reversals in the differences occur as well. Such reversals are possible, despite greater

topographic obstruction at lower elevation, because the effects of sunlight reflection from the surrounding topography, and of cloud cover, can be highly variable within the glacier basin. To the extent that the short-wave radiation environment can be characterized as one of extremes, this is evident in the results as well.

The definition of short-wave reflectivity and incorporation of the Stefan-Boltzmann law for radiation allow Equation (2) to be changed into a form that demonstrates the importance of radiative inputs and surface characteristics to the net radiation:

$$Q_* = K\downarrow (1 - \alpha) + L\downarrow - \varepsilon_s \sigma T_s^4 \qquad (3)$$

The Equation underlines the importance of ensuring that automatic weather stations have the capacity to record solar radiation and that if atmospheric radiation records cannot be included among the measurements, then effective steps must be taken to estimate $L\downarrow$ from air temperature data (Idso and Jackson, 1969; Oke, 1987). As to surface reflectively and emissivity, α is by far the most variable over the glacier basin (Cutler, 2006), thus underlining the need for further field work of the type described in Cutler and Munro (1996) and for extension of the satellite work described in Gratton *et al.* (1994).

Turbulent transfer components

The bulk transfer approach to turbulent heat flux estimation has been tested against eddy correlation measurements at Peyto Glacier (Munro, 1989) and found to work well if care is taken to provide adequate estimates of surface roughness and to correct for atmospheric stability. The approach has proven to be useful at Peyto (Munro, 1990) and elsewhere (van den Broeke, 1996a). The essentials of the method are stated here.

Estimates of Q_H and Q_E are obtained from measurements of wind speed, u, air temperature, T, and vapour pressure, e, taken at height, z = 1 m above the melting surface:

$$Q_H = \rho c_p k^2 u T([ln(z/z_o) + 5z/L][ln(z/z_t) + 5z/L])^{-1} \qquad (4)$$

$$Q_E = (\rho \varepsilon L_v k^2 \, u[e\text{-}e_s]/p)([ln(z/z_o) + 5z/L][ln(z/z_e) + 5z/L])^{-1} \qquad (5)$$

in which ρ is air density, c_p the specific heat of air at constant pressure, k von Kàrmàn's constant, L the Monin-Obukhov stability length scale, ε the molecular weight ratio of water to that of dry air, L_v the latent heat of vapourization, e_s the surface vapour pressure, p the air pressure, z_o, z_t and z_e, respectively, the surface roughness lengths for wind speed, air temperature and vapour pressure.

The use of the Monin-Obukhov length for stability correction distinguishes this approach from the more frequently applied Richardson number scheme (Föhn, 1973; Moore, 1983). It is calculated from

$$L = \rho u_*^3 T \left(kgQ_H\right)^{-1} \qquad (6a)$$

where g is the gravitational acceleration, u_* the friction velocity, and T is expressed in degrees Kelvin. Equation (6a) suffers from the obvious problem that L is initially required for the calculation of Q_H and u_*:

$$u_* = ku[ln(z/z_o) + 5z/L]^{-1} \qquad (6b)$$

The problem is resolved by first estimating Q_H from Equation (4) for the neutral stability case, where 5 z/L is zero, then calculating first estimates for L and u_* from Equation (6b). The procedure continues iteratively until there is no further significant change in Q_H, usually after three iterations. The stability correction can reduce estimated sensible heat flux to the melting surface to 80% of what it would otherwise be (Munro, 1989), and so constitutes a significant correction.

It is also crucial to estimate z_o for a specific site, a task which is most practically accomplished by the Lettau (1969) method of roughness element description:

$$z_o = 0.5h^*s/S \qquad (7)$$

where effective roughness element height, h^*, silhouette area, s, and element density, S, can be established from micro-relief description (Weller, 1968; Föhn, 1973; Munro, 1989). The result is a fixed value of aerodynamic roughness which is used in expressions for the more dynamic temperature and vapour pressure counterparts (Andreas, 1987):

$$z_t = \exp\left[ln(z_o) + 0.317 - 0.565\ ln(Re_*) - 0.183(ln[Re_*])^2\right] \qquad (8a)$$

$$z_o = \exp[ln(z_o) + 0.396 - 0.512\ ln(Re_*) - 0.180(ln[Re_*])^2] \qquad (8b)$$

where the kinematic viscosity of air, n, is used in the calculation of the roughness Reynolds number, $Re_* = u_*\ z_o/\nu$. Aerodynamic roughness length estimates for Peyto are 2.5 mm for ice (Munro, 1989), 5 mm for snow (Föhn, 1973).

Energy Components of Melting Ice and Snow

A five-day sequence of air temperature, vapour pressure and wind speed at an ice site on the glacier tongue is plotted in Figure 6. It was recorded during a change from fair, sunny weather to poorer weather conditions, during which field notes indicate rainy periods for June 28 to 29. Corresponding changes to the boundary-layer environment over ice indicate a cooling trend in the air temperature, as well as vapour pressures that change from less, to more than the ice point value (Figure 6). Wind speed varies from 2 to 6 m s^{-1} during that period, the stronger winds occurring near the beginning.

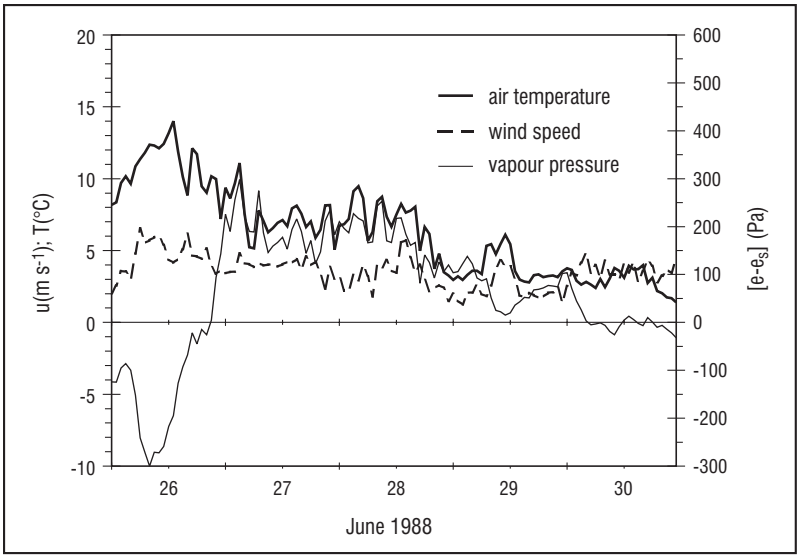

Figure 6. *Five day series of boundary layer properties at 1 m above melting ice on the tongue of Peyto Glacier. Notation is defined in text.*

Concurrent data to use in calculating mean daily total energy inputs and mean hourly values of short-wave reflectivity, air temperature, vapour pressure and wind speed for the ice site, and for the snow site, were obtained for a fifteen day period (Table 3). They indicate that a slightly lower solar radiation income for ice than for snow is strongly offset by the much lower reflectivity of the ice. The daily input of atmospheric radiation clearly exceeds that of solar radiation, but it is more than offset by the expected daily long-wave loss of 26.7 MJ m^{-2} from a melting surface. Although the result is a net long-wave radiation loss, the large size of the long-wave input illustrates why potential responses of $L\downarrow$ to climate change must be considered in assessments of glacier fluctuations (Oerlemans, 1986, 1988).

Wind speed is stronger over ice than over snow, a consequence of acceleration down-glacier in katabatic flow. Mean temperature and vapour pressure are greater than melting point values at both sites, thus indicating sensible and latent heat transfer from air to surface. This would be expected to result in cooling and drying of the air as it moves down the glacier from snow to ice, an outcome which seems to be confirmed for humidity by the slightly lower vapour pressure over ice. The outcome is also confirmed for air temperature by noting the dry adiabatic adjustment of -0.01°C m^{-1} which must be included to compare potential temperature contrast across the 270 m elevation difference between the sites. This changes an apparent down glacier warming of 1.67°C to a cooling of -1.03°C.

Table 3. *Mean daily total energy inputs and mean hourly albedo, air temperature, vapour pressure and wind speed, June 22 to July 8, 1988, Peyto Glacier (Munro, 1990).*

SURFACE	ELEVATION(m)	K↓(MJ m^{-2})	L↓(MJ m^{-2})	α	T(°C)	e(Pa)	u (m s^{-1})
Ice	2240	15.0	25.3	0.357	5.40	648	3.56
Snow	2510	17.2	24.3	0.728	3.73	660	2.98

Flux density variations of melt energy components

Hourly variations of net radiation, sensible heat exchange and latent heat exchange due to water vapour show the dominance of net radiation in the melting of glacier ice (Figure 7a). Sensible heat exchange is a smaller, persistent supplier of energy to the surface. Latent heat exchange associated with the vapour flux density begins as a small energy loss due

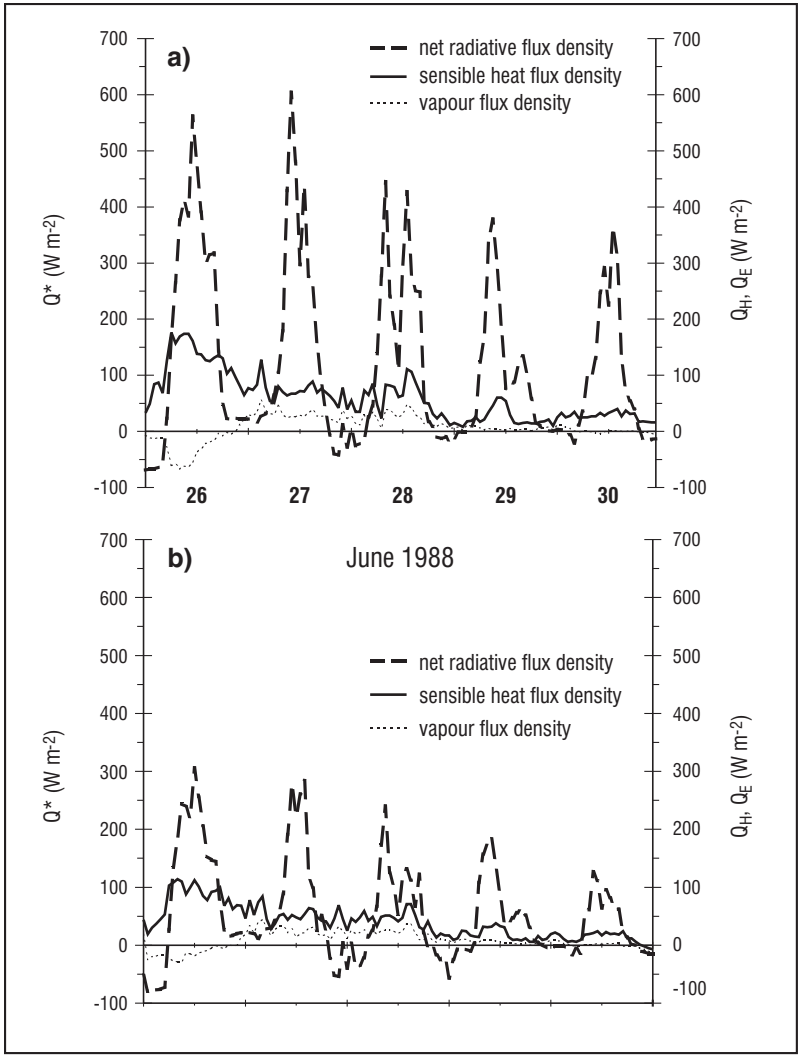

Figure 7. *Energy exchange components during melt conditions at Peyto Glacier for a) ice on the glacier tongue; b) snow in the glacier upper basin.*

to evaporation, but it soon changes to a small energy gain through condensation. Reversal in the direction of Q_E appears to be associated with deteriorating weather over the five day period, which also marks a general decrease in energy supply to the ice.

The energy exchange for melting snow (Figure 7b) is similar to that of ice, except that net radiation income is much reduced by the greater reflectivity of snow and, to a lesser extent, the smaller income of atmospheric radiation (Table 3). In fact, the reduction is such that Q^* is no longer the most important contributor to melt energy (Table 4), a result which has also been reported elsewhere, more recently during the onset of melt in Greenland (Stefan, 1995). As is the case for ice, the turbulent transfer terms at night may supply sufficient energy to compensate for net radiative loss, particularly under cloud cover. Despite the fact that the greater roughness length of snow has the potential to induce greater turbulence, the smaller wind speeds and air temperatures result in less Q_H for snow than for ice.

Table 4. *Mean daily total components of melt energy supply, QM (MJ m^{-2}) to snow and ice on Peyto Glacier, June 22 to July 8, 1988 (Munro, 1990).*

SURFACE	K_*	L_*	Q_*	Q_H	Q_E	Q_M
Ice	9.65	-1.40	8.25	4.44	0.410	13.1
Snow	4.68	-2.40	2.38	2.73	0.470	5.48

The importance of snowline migration to glacier meltwater production can be appreciated by comparing the mean daily totals of energy transfer for ice and snow (Table 4). According to this example, the removal of snow cover doubles the capacity of the glacier to absorb sunlight, which accounts for most of the Q_M increase for ice over snow. The change to ice probably increases local variability in meltwater production as well because there is significant local variability in ice reflectivity (Cutler and Munro, 1996; Cutler, 2006), which has been shown to explain variability in ice ablation (van de Wal *et al.*, 1992). Meltwater production over the whole glacier can therefore exhibit marked contrasts between low and high snow line years.

The timing of first ice exposure during the ablation season will depend upon the thickness of the winter snow pack and upon weather conditions near the beginning of the season. It is readily appreciated that a thin winter snow pack points toward early exposure of the ice. It is not so clear that

cloudy weather is likely to be more suitable for early exposure than is sunny weather until one considers the 'radiation paradox' (Wendler, 1986) in light of the contents of Tables 3 and 4.

Previous investigations at Peyto Glacier indicated that solar radiation under overcast sky was likely to be approximately half the value to be expected under a clear sky (Munro and Young, 1982). If one assumes that variable cloud conditions over the June 22 to July 8 period place $K\downarrow$ values in Table 3 between those extremes, at three quarters of clear sky values, then it follows that K_* under overcast sky would fall to two thirds of the values stated in Table 4. Taking further assumptions that overcast sky reduces L_* virtually to zero at both locations, without affecting the turbulent transfer terms, Q_M falls from 13.1 to 11.3 MJ m^{-2} over ice, but rises from 5.48 to 6.30 MJ m^{-2} over snow.

If overcast skies are identified with bad weather, clear skies with good weather, then a strong ablation year is likely to be one in which the bad weather occurs early, rather than later in the melt season. Given the potential for a strong ablation year to force a negative net mass balance, and the ability of cloud cover to raise T_{min}, one is left with a physical mechanism to explain Letréguilly's results (Table 2). Additionally, one must consider the potential for rain falling on a ripe snow pack to accelerate the process.

Comparison of water equivalents with ablatometer measurements

The water equivalent of ablation due to melt is estimated from Equation (1). Attempts to validate the results against ablation measurements tend to give encouraging results for daily totals (Müller and Keeler, 1969; Föhn, 1973; Munro, 1990). The work of Müller and Keeler (1969) was particularly notable for its attention to the development of the weathering crust but, as was the case for Föhn (1973), closure between estimate and measurement was achieved by adjusting the turbulent transfer coefficients.

In Munro (1990) the development of the estimation procedure was kept independent of the measurements themselves, which were facilitated by the use of the Lewkowicz (1985) ablatometer (Figure 4b). The sensing element of this device is a potentiometer, linked to a moveable metal tube, supported between two poles which are drilled at least 2 m into the surface to minimize subsidence of the supports. The sensing tube has a foot

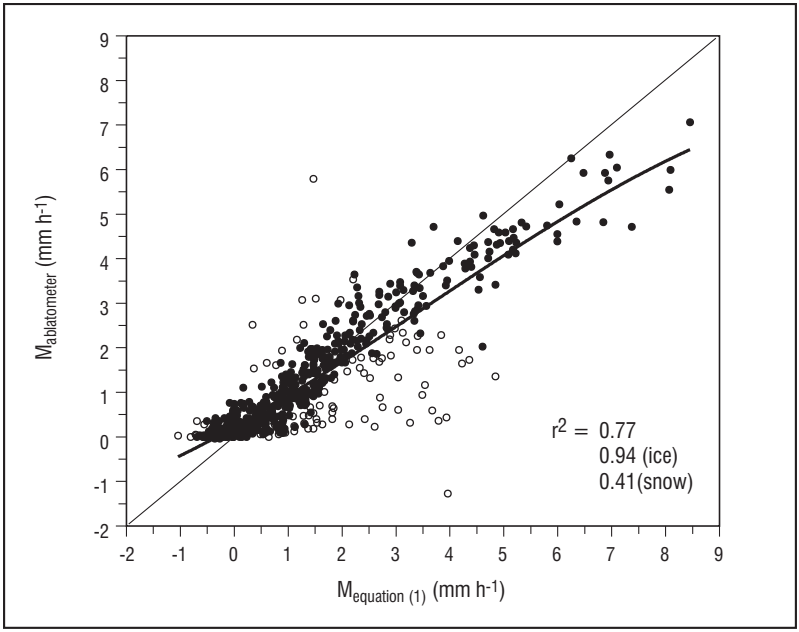

Figure 8. *Hourly melt comparisons for ice (closed circles) and snow (open circles), with third order polynomial fit and 1:1 line.*

constructed of wood for ice, plastic for snow, which rests on the surface, thus following it down as ablation occurs. Good agreement between daily *M* totals from these devices and *M* from micro-meteorology (Equation 1) has been obtained for ice, fair agreement for snow (Munro, 1990).

As encouraging as reasonable agreement for daily totals may be, a more demanding test is to compare the hourly values (Figure 8). The comparison shows remarkably good agreement for ice ablation, particularly in the 1 to 4 mm h^{-1} range. Overestimates tend to occur above that range, while underestimates tend to occur below, such that negative values are indicated for night data. The extreme outliers among the results tend to be associated with snow ablation, where significant error occurs by assuming a constant snow density with depth, thus ignoring the presence of ice layers in the snow pack.

The tendency for energy component estimates of ablation to be too large toward the high end of the data range, and too small at the low end, is consistent with the description of weathering crust development outlined

in Müller and Keeler (1969). They showed that days of overestimation were likely to be those marked by fair, sunny weather, when differential melting within the surface could occur without a corresponding amount of surface lowering. Under cloudy skies, the structure left behind by the sunny periods would tend to break down, resulting in rates of surface lowering which seemed to exceed the amounts of energy provided for melt. The result depicted in Figure 8 is entirely consistent with their description of weathering crust development, except that diurnal variation in net radiation is the controlling factor here.

Further Consideration of the Glacier Cooling Effect

It is apparent from the work of van den Broeke (1997a, b) that a clear understanding of turbulent energy transfer to the glacier surface requires one to consider the adiabatic heating of the air as it moves down glacier. As noted with respect to the mean temperatures in Table 3, the cooling effect of the glacier remains hidden in the data unless this is taken into account. It is particularly instructive in this regard to reexamine the data presented by Foessel (1974) in his study of the temperature distribution over Peyto Glacier.

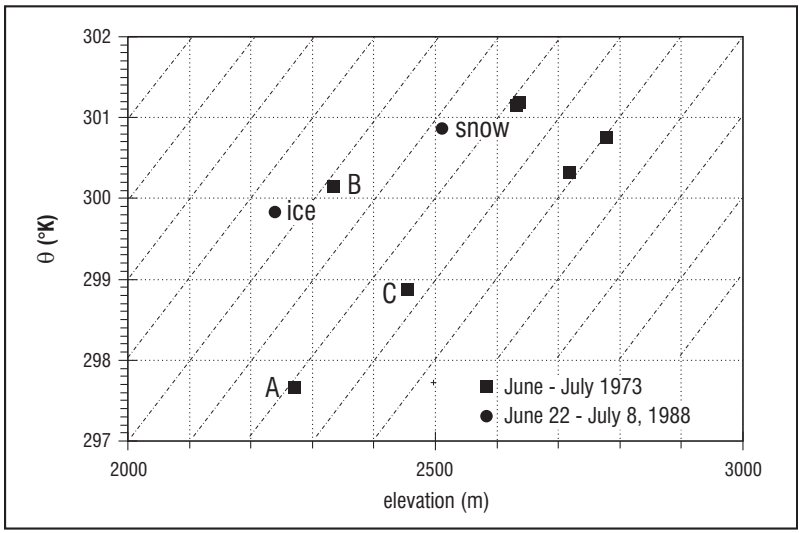

Figure 9. *Potential temperature, θ, at various elevations on Peyto Glacier, derived from data in Foessel (1974) and in Table 3. Sloping lines are dry adiabats.*

Foessel recorded the 1.5 m air temperature at a number of locations in the glacier basin, some of which could be used to estimate the background air temperature of the area around the glacier. Mean hourly temperatures were calculated for day and night periods in the months of May, June, July and August. Day and night periods were consistent in showing a fall in the environmental temperature with increasing elevation, the size of the lapse rate varying from one set of station comparisons to the next. A different picture emerges if Foessel's results are adiabatically corrected to potential temperature at 100 kPa (Figure 9).

When considered within the context of down glacier air flow, the results demonstrate a general cooling of the glacier boundary-layer as the air moves to lower elevations, a result which is consistent with findings on Pasterze Glacier (van den Broeke, 1997a, b). Similarly, the cooling effect is evident in comparing the ice and snow site results in Table 3 after adiabatic corrections have been applied to the air temperature data (Figure 9). In fact, the comparison between potential temperatures obtained from Table 3 and those obtained from Foessel (1974) is remarkably close despite the fact that neither similar observation periods nor similar air temperature sensors were used in the two studies.

The fact that the points plotted in Figure 9 show what appear to be warm or cold deviations from any straight line which might be drawn through the results affirms that flow connections between different points are not necessarily direct. Nevertheless, stations at the lowest three elevations on the plot of Foessel's results (Figure 9: A, B, C) are sufficiently close to the glacier centre line to invite speculation as to how such deviations could occur. Foessel (1974) had interpreted this in terms of colder air pooling at specific locations on the glacier, thus creating 'cold spots' (Figure 9: A, C).

One way to view such an interpretation is to consider the possibility of cold or warm temperature deviations due, respectively, to horizontal convergence or divergence within the katabatic flow field above the glacier. There is already horizontal divergence along any streamline of the katabatic wind because it continues to accelerate down glacier, thus setting the stage for the air above to subside and to carry with it the sensible heat which has been entrained from the anabatic flow field (Figure 3). Because the katabatic flow field at a given height above the glacier comprises any number of streamlines which originate from an extensive upper basin, they may converge laterally across the flow field in areas where the glacier narrows and separate where it broadens out (Figure 10).

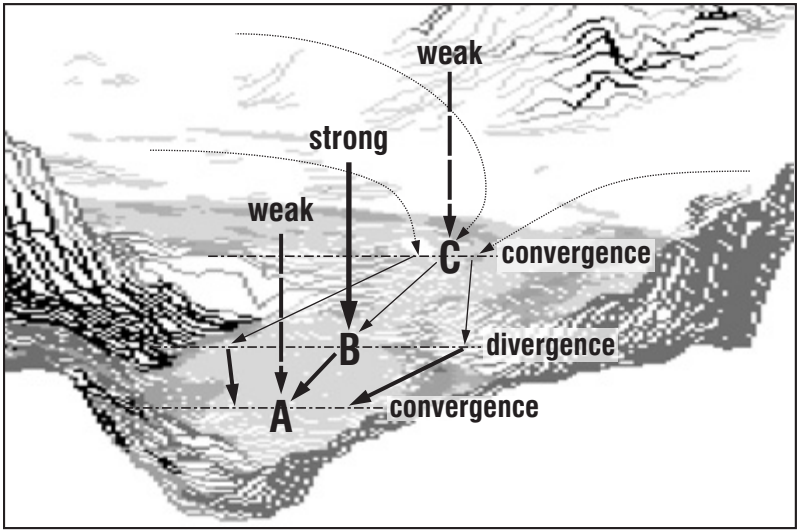

Figure 10. *Lateral convergence and divergence scheme, with associated weak and strong subsidence of warm air from anabatic flow field above, resulting in relatively cooler boundary layer conditions at* ***A*** *and* ***C*** *than at* ***B****.*

Lateral convergence can be compensated by additional acceleration of the glacier wind. But there is also likely to be some associated upward motion which weakens the subsidence, thus reducing heat delivery toward the surface, the result being a relatively cold temperature deviation. Where the flow separates laterally one may expect the reverse: a weakening of down glacier flow acceleration, strengthened subsidence, additional heat delivery, and a relatively warm temperature deviation.

The 1988 data allow examination of the cooling effect in more detail, on an hourly basis. Hourly differences between snow and ice site temperatures and wind speeds, with adiabatic adjustment, are plotted over the June 26-30 period (Figure 11). Acceleration of the air moving down glacier tends to be strongest during the daylight hours, when the temperature contrast between the glacier and its surroundings is likely to be best developed. Smaller accelerations, in fact some decelerations as well, tend to occur at night, a somewhat surprising result in view of the Pasterze Glacier findings, where the changeover from anabatic to katabatic valley flow at night reinforces the glacier wind (van den Broeke, 1997a). Although the wind speed difference pattern seems to correspond with the

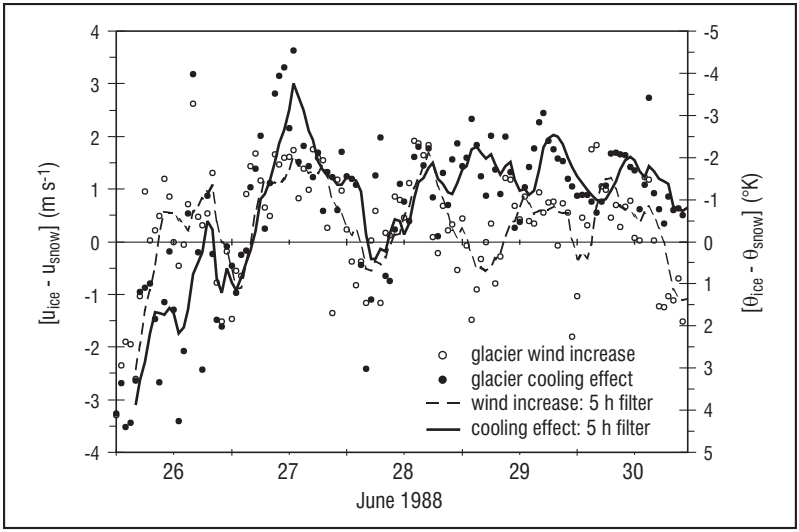

Figure 11. *Down glacier wind speed increase and cooling effect. Potential temperature axis is inverted to depict both acceleration and cooling effect as increasing upward on the diagram.*

temperature difference pattern over the first half of the sequence, such that increases in acceleration tend to be matched by increases in cooling, the correspondence breaks down over the latter half. This may signify that the cooling trend in temperature recorded over that period (Figure 5) eventually reaches the stage where there is no longer sufficient temperature contrast between the glacier and its surroundings to maintain the system.

Another approach to the glacier cooling effect is to apply the results stated in Tables 3 and 4 to a suitable arrangement of the heat storage Equation, from which to estimate the thickness, ΔZ, of cooled air adjacent to the glacier surface:

$$\Delta Z = \Delta t Q_H (\rho c_p \Delta\theta)^{-1} \qquad (9)$$

in which $\Delta\theta$ is the potential temperature change between upstream and downstream locations, and Δt is the travel time between locations. An approximate travel time of 550 s between snow and ice locations is estimated by dividing the 1800 m distance which separates them by the

mean of the two wind speeds in Table 3. Then, taking ρc_p to be approximately 1000 J m^{-3} K^{-1} , $\Delta\theta$ = -1.03°K, and expressing the average of the two sensible heat components in Table 4 as a boundary layer heat loss, Q_H = - 41.5 J s^{-1} m^{-2}, a cooling layer thickness in the order of 20 to 25 m is obtained. This is comparable to the 20 m thickness suggested for Pasterze Glacier (van den Broeke, 1997b).

MODELLING GLACIER RESPONSES TO THE WEATHER

Diagnostic Glacier Response Modelling

A simple, yet extremely interesting model was outlined by Oerlemans (1986), to address the question of glacier sensitivity to increasing 'greenhouse' gas accumulation in the atmosphere. The main focus was upon the augmentation of atmospheric long-wave radiation and its effect on ablation, but a truly exciting feature of the model was the consideration of horizontal heat exchange between the glacier boundary layer and that of the surrounding land. The modelling scheme demonstrated that glacier extent is an important determinant of its sensitivity to environmental change. Glaciers such as Peyto, Pasterze and White Glaciers, which span distances of 5 km or more from beginning to end, are probably sufficiently large to develop boundary layer climates that are distinct from those of their surroundings. Thus, they are likely to exert a stronger cooling effect upon the air above than would a smaller glacier like Ram, Sentinel or South Cascade Glacier.

Oerlemans' model was modified for application to the altitudinal distribution of Peyto Glacier mass balance data (Young, 1981) in such a way that it was possible for the model to generate snowline migration during the ablation period, given the winter mass balance distribution (Munro, 1991). One consequence of the exercise is the ability to demonstrate the sensitivity of minimum seasonal snow cover area on the glacier to variations in the atmospheric environment, surface reflectivity and solar radiation (Table 5).

The results are useful in diagnosing various possibilities for glacier mass balance fluctuations, despite the simplicity of the modelling approach. The parameters listed in Table 5 are among the most frequently postulated agents of global change, not the least of which are the small effects of

Table 5. *Peyto Glacier snow cover responses to changes in selected atmospheric and surface parameters, where snow initially covers 52% of the glacier surface at the end of the ablation season (Munro, 1991).*

INITIAL PARAMETER VALUE […]	Ratio of glacier snow cover area to initial area of 52%				
atmospheric emissivity [0.80]	1.62	1.35	1.00	0.85	0.33
air temperature [270°K]	1.40	1.08	1.00	0.94	0.71
surface reflectivity [0.65]	0.31	0.85	1.00	1.37	1.65
solar constant [1367 W m^{-2}]	1.46	1.19	1.00	0.90	0.56
Change Relative to Initial Value	*-5%*	*-1%*	*0%*	*1%*	*5%*

Milankovitch cycles on solar radiation (Crowley and North, 1991). There is almost a twenty percent snow area increase suggested for only a one percent fall in the value of the solar constant. The contention of Oerlemans (1986), that glaciers can be extremely sensitive to atmospheric emissivity, stands out well in the results, but the point is also made that a truly effective assessment of any particular glacier requires precise determination of surface reflectivity, especially if the objective is to model meltwater production from glaciers.

Operational Glacier Response Modelling

A model becomes operational when it can turn continuous inputs of information, such as weather data, into continuous predictions, such as the changes to expect in glacier mass balance and associated meltwater production. This changes the nature of the model from that of a diagnostic exercise into that of a forecasting tool. The construction of a primitive model for Peyto Glacier begins by incorporating the modelling elements described in Munro (1991) and using weather station data, $K\downarrow$ and T_a, to drivea model that continually resets glacier air temperature, T, and surface temperature, T_S (Table 6).

The modelling scheme outlined in Table 6 is geographically primitive because glacier topography is lumped into elevation zones, but it does include the different reflectivities of ice and snow. The key to making the model work with data is to note that clear sky models of solar radiation (Munro and Young, 1982) and atmospheric emissivity (Idso and Jackson, 1969; Deacon, 1970), define the upper limit of $K\downarrow$ and the lower limit of $L\downarrow$ (Figure 12). Then it becomes possible to use $K\downarrow$ data, which are relatively easy to measure at a field station, to solve iteratively for cloud

amount, n (Table 6). The value for n is incorporated into the model for $L\downarrow$, a quantity for which data are seldom available. Station air temperature data, T_a , provide air temperature estimates for the glacier surroundings from which to model $L\downarrow$.

The scheme is also meteorologically primitive because much that is meteorologically correct is ignored. Q_H is calculated without stability correction, thermal roughness or glacier wind model, thus necessitating the use of weather station data for wind speed. Station air temperature is assumed to represent cloud base temperature, even though this is expected to be cooler at cloud base elevation, and cloud cover is fixed at one value throughout the day (Figure 12). Furthermore, the use of solar radiation data to estimate could cover requires the assumption that cloud cover during daylight hours represents entire 24 hour periods, an assumption which is highly suspicious, especially for days when a fair weather cumulus cloud regime is established.

Table 6. *A primitive melt modelling scheme for Peyto Glacier, in which d is the surface layer thickness, h the boundary layer thickness, A the glacier area (where subscript, j, denotes elevation zone), T_g the sub-surface temperature, κ_x a horizontal heat transfer coefficient ε_a the atmospheric emissivity, τ is the day length, and remaining notation is defined in the text. Model time step, Δt, is set to one hour.* ***Bold face*** *denotes measurement input.*

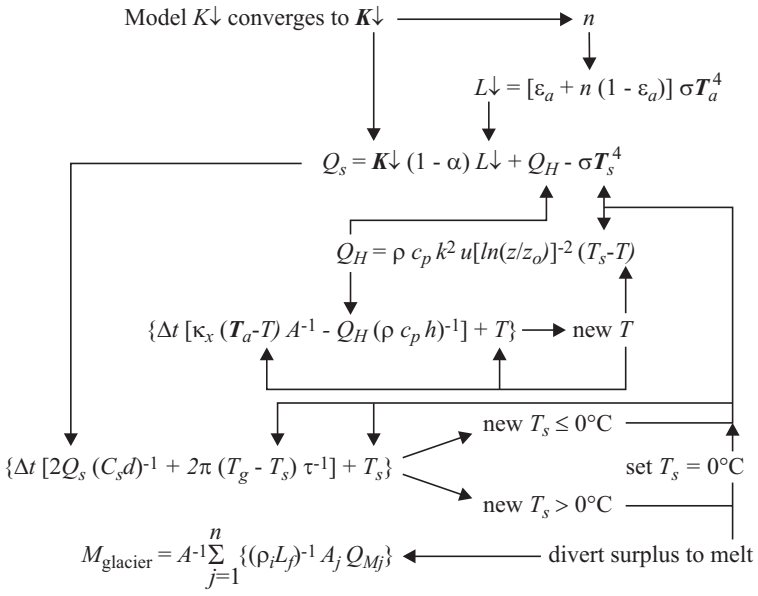

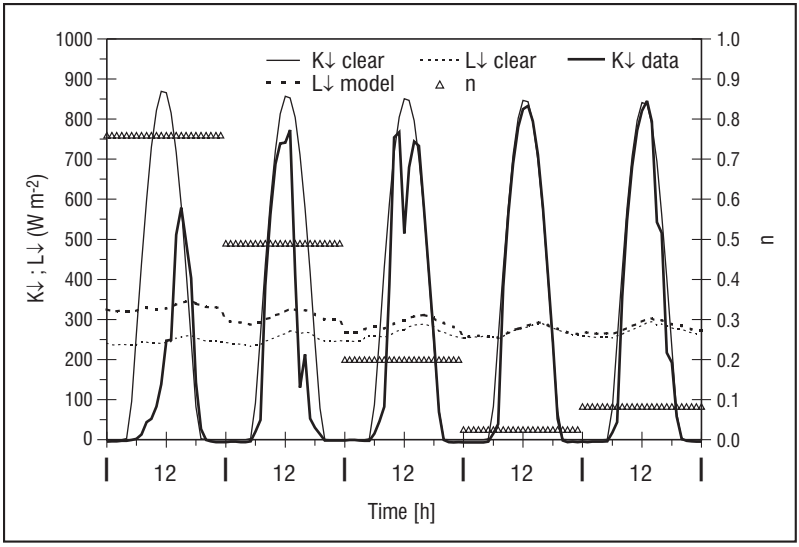

Figure 12. *Five-day radiation modelling sequence, taking the example of solar radiation data from Place Glacier, August 1991. All other quantities are model estimates.*

A further cautionary note to sound about the modelling scheme is that the decision has been made to use temperature as a switch to activate melt and rain events. Melt events are activated by surface temperature, rather than air temperature, thus allowing surface melt to occur in sub-freezing air temperatures, as suggested in Kuhn (1987), but it does not allow for sub-surface melt adjacent to the frozen top of a snow pack (Colbeck, 1982). Air temperature is the switch for precipitation, arbitrarily set to indicate rain for $T_a > 0$°C, snow for $T_a \leq 0$°C. Because T_a plays such a prominent role in modelling atmospheric radiation, one should also consider that the glacier cooling effect may cause T_a to deviate from the temperature of its surroundings, with the consequence that $L\downarrow$ may be underestimated (Meesters and van den Broeke, 1997).

Despite its limitations, the model yields interesting results for meltwater production during the ablation season and for snow pack development during the accumulation season.

Meltwater production

The key driving variables for meltwater production are solar radiation and station air temperature. Precipitation is not included because the objective is to examine the melt response to weather variations solely in connection with ablation. The incorporation of cloud cover estimates to augment $L\downarrow$ is extremely important to the predicted outcome of the melt response, as can be seen by comparing it to the outcome when temperature alone is used to estimate $L\downarrow$ (Figure 13). Failure to include cloud cover delays the onset of melt until June, well after it is already known to be active in ripening the snowpack. Furthermore, although the end of September is a reasonable time to begin the winter snow cover, it would also be reasonable to expect small melt events through the month of October, such as those which are indicated when the effect of cloud cover upon $L\downarrow$ is included.

Another feature of interest is the considerable lag in melt response. Peak melt predictions occur in August, well after the annual solar maximum. Station temperature demonstrates a similar lag response. The peaks come at a time when seasonal reduction in $K\downarrow$ is more than offset by the effects

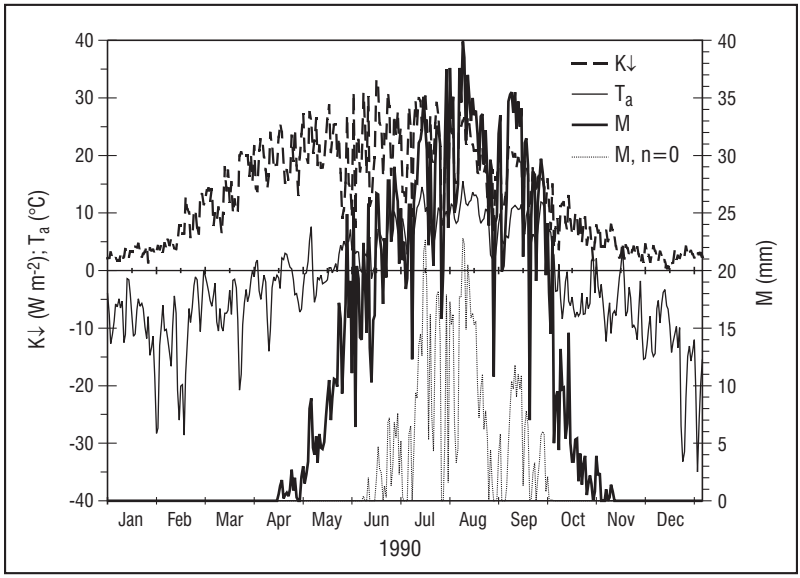

Figure 13. *Meltwater simulation sequence, showing M with and without (n = 0) the effect of cloud.*

of snowline retreat on surface short-wave reflectivity, a time when large areas of exposed glacier ice maximize the capacity for the glacier to act as a solar collector. The effects are manifest in the glacier surroundings as warmer air temperature data because the cooling effect of seasonal snow cover is minimal at this time.

This helps to explain why temperature index approaches to the prediction of meltwater yield from glacierized basins can be quite effective. Success occurs not so much because of the ability for T_a to represent heat transfer from air to ice, but because ablation and air temperature are co-respondents to the changing capacity of the basin to absorb solar radiation. The correspondence between temperature and melt responses to radiation is likely to be poorer in mid-day than at other times, because daytime ice melt responds very quickly to sunlight. This may further explain why Letréguilly (1988) achieved less success with maximum than with minimum temperature explanations of summer mass balance.

Snow pack development

Excavations of snow pits to measure the winter mass balance of a temperate glacier usually display dense strata in the snow pack, layers which have been modified by winter rain and melt events. This speaks to a complex seasonal history of snow pack development that can be explored by combining base camp precipitation data with elements of the melt modelling scheme outlined in Table 6.

Some caveats apply. The most important of these to bear in mind is that although gauge catch corrections (Goodison *et al.*, 1981) have been applied to the data, there is no confirmation that either the corrections or the gauge location itself are suitable for providing accurate estimates of precipitation input to the glacier surface. In fact, they cannot be accurate without accounting for sublimation loss from blowing snow (Pomeroy, 1991), a factor which is not considered here. Neither, for that matter, is sublimation loss from or condensation gain to the snow pack itself taken into consideration, nor are any of the processes associated with snow metamorphism (Colbeck, 1982).

Caveats noted, it is clear from snow pit excavations on the glacier tongue and from the weather records that the timing of accumulation season melt and precipitation events is useful in interpreting snow pack development

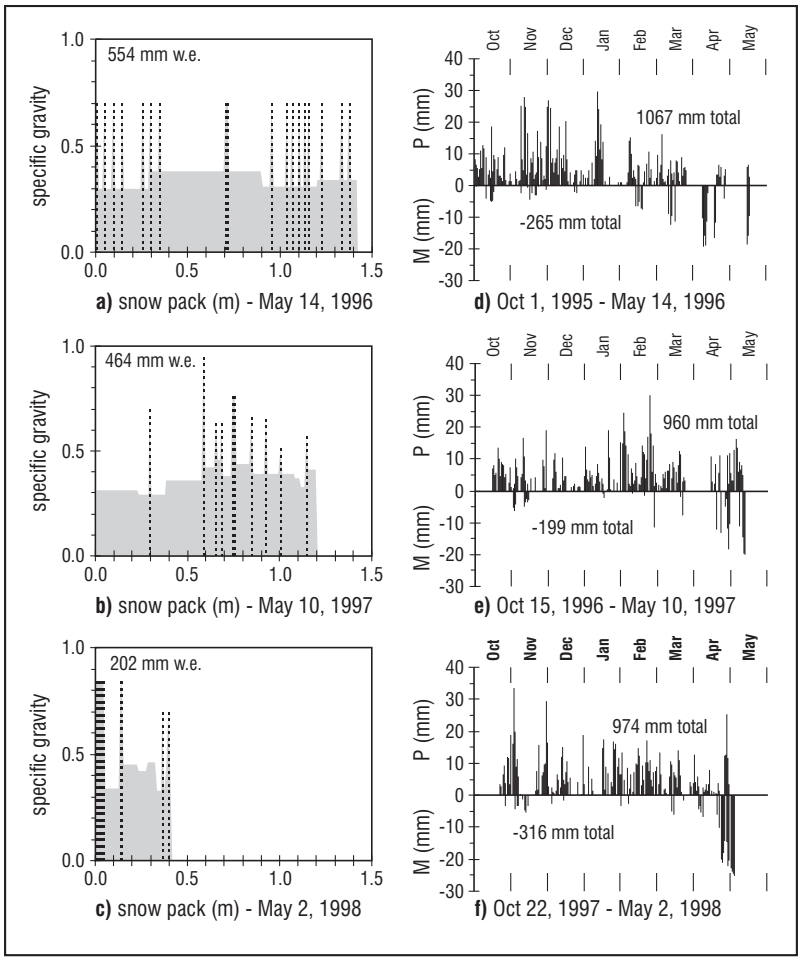

Figure 14. *Snow pack density profiles (dense lenses portrayed as broken bars) obtained on the tongue of Peyto Glacier, with antecedent precipitation and modelled melt records dating from estimated beginning of the accumulation phase.*

(Figure 14). The 1995-96 record (Figure 14d) shows that snow cover was firmly established at the beginning of October, and that a number of precipitation events, interspersed with melt events and probable rain (melt conditions imply rain when they coincide with precipitation), occurred through the following 60 days. Substantial amounts of precipitation were

delivered in December and January, but little melt occurred until February, when the regime changed to one of smaller precipitation events and intermittent melt events. Because the 0°C isotherm was near the snow surface at the time of excavation, this weather sequence is captured in the snow pack (Figure 14a). The fact that the recorded precipitation total of 1067 mm water equivalent is approximately twice the amount stored in the snow pack (554 mm) attests to the concerns about gauge accuracy and loss from blowing snow expressed above.

CONCLUSION

Micro-meteorological investigations at Peyto Glacier provide a firm basis for understanding the energetics of the ablation phase of the mass balance cycle, as well as guidance about how to proceed with the accumulation phase. Winter climate research is not extensively reported in the literature on valley glaciers, certainly not in the detail devoted to some aspects of avalanche forecasting (Brun *et al.*, 1989). More attention should be directed toward it because, as important as surface energy exchange is during the ablation season, weather station records indicate that it is also an important aspect of the accumulation season. One of the important contributions of such work would be to more precisely establish the timing of minimum and maximum mass balance, an important aspect of interpreting the role of seasonal influences on glacier mass balance.

A productive starting point at Peyto would be to place less emphasis upon summer research work and move much of the field effort into the autumn and spring. This would provide detailed documentation of the transition periods between the ablation and the accumulation phases of the mass balance cycle. The timing of the transition periods, the associated changes in surface characteristics, and a clear understanding of the mechanisms at work, are crucial to understanding mass balance fluctuations and their implications for glacier hydrology.

There is currently the great advantage that field studies can be placed in the context of the automatic weather station record. That record is now approaching one decade in length, a sufficiently long period of time to consider a comparative climatology with other stations in the area, perhaps to sharpen our knowledge of what has been gained from synoptic and statistical analysis of glacier response to climatic variation. The existence of the station also means that prospects for modelling an energy balance

climatology of the basin to use for interpretation of mass balance variations, and their impacts upon local water supply (Meier, 1969), are currently stronger than ever before. The key to realizing these prospects is to employ knowledge of the surface energy exchange processes which are at work to effectively model the link between weather variations and glacier mass balance fluctuations.

ACKNOWLEDGEMENTS

Most of the climatological field work over the years has been financially supported by the Natural Sciences and Engineering Research Council of Canada, and conducted in partnerships with the National Hydrology Research Institute, the National Glacier Programme of the Geological Survey of Canada and with the permission of Parks Canada. Recently, financial support has also been obtained from the Meteorological Service of Environment Canada, as part of current efforts to develop a Cryospheric System to monitor global change in Canada. Ideas for this chapter were initially presented at the Peyto Glacier 100th Anniversary Workshop. Revisions to the original manuscript have benefited from the reviews of Graham Cogley and Andrew Fountain.

A special note of thanks is expressed to Wayne Rouse, Tim Oke and John Davies for getting me started in climatology, to Leo Derikx, who first directed my attention toward glacier hydrology, to Tijs Bellaar-Spruyt for my first lessons on glacier field research management, and to my field assistants over the years: Barbara Alberton, Trevor Bain, Donald Chisholm, Peter Duck, Andrew Munro, Nora Munro and Catherine Samuels. My graduate students, Paul Cutler, Andrew Lowe and Gary Grant assisted me as well. Appreciation is also expressed to Adam Munro for initial preparation of the diagrams, and to Lisa Munro for being there at the beginning.

REFERENCES

Alt, B.T. 1987. Developing synoptic analogues for extreme mass balance conditions on Queen Elizabeth Island ice caps. *Journal of Climate and Applied Meteorology* **26**(12): 1605-1623.

Ambach, W. 1974. The influence of cloudiness on the net radiation balance of a snow surface with high albedo. *Journal of Glaciology* **13**(67): 73-84.

Andreas, E.L. 1987. A theory for the scaler roughness and the scaler transfer coefficients over snow and sea ice. *Boundary-Layer Meteorology* **38:** 159-184.

Brun, E., E. Martin, V. Simon, C. Gendre and C. Coleou. 1989. An energy and mass model of snow cover suitable for operational avalanche forecasting. *Journal of Glaciology* **35**(121): 239-248.

Braithwaite, R.J. and O.B. Olesen. 1990a. Response of the energy balance on the margin of the Greenland ice sheet to temperature changes. *Journal of Glaciology* **36**(123): 217-221.

Braithwaite, R.J. and O.B. Olesen. 1990b. A simple energy balance model to calculate ice ablation at the margin of the Greenland ice sheet. J*ournal of Glaciology* **36**(123): 222-228.

Bücher, A. and J. Dessens. 1991. Secular trend of surface temperature at an elevated laboratory in the Pyrénées. *Journal of Climate* **4**(8): 859-868.

Colbeck, S.C. 1982. An overview of seasonal snow metamorphism. *Reviews of Geophysics and Space Physics* **20**(1): 45-61.

Crowley, T.J. and G.R. North. 1991. *Paleoclimatology*. Oxford University Press, 349 p.

Cutler, P.M. and D.S. Munro. 1996. Visible and near-infrared reflectivity during the ablation period on Peyto Glacier, Alberta, Canada. Journal of Glaciology **42**(141): 333-340.

Deacon, E.L. 1970. The derivation of Swinbank's longwave radiation formula. *Quarterly Journal of the Royal Meteorological Society* **96:** 313-319.

Demuth, M.N. and R. Keller. 2006. An Assessment of the Mass Balance of Peyto Glacier (1966-1996) and its Relation to Recent and Past-century Climatic Variability. In: *Peyto Glacier: One Century of Science.* Demuth, M.N., D.S. Munro and G.J. Young (eds.). *National Hydrology Research Institute Science Report* **8**: 83-132.

Derikx, L. 1975. The heat balance and associated runoff from an experimental site on the glacier tongue. *International Association of Scientific Hydrology Publication* **104:** 59-69.

Foessel, D.G. 1974. An analysis of the temperature distribution over the Peyto Glacier, Alberta. *M.Sc. Thesis*, University of Guelph, 137p.

Föhn, P.M.B. 1973. Short-term snow melt and ablation derived from heat and mass balance measurements. *Journal of Glaciology* **12**(65): 275-289.

Goodison, B.E., H.L. Ferguson, and G.A. McKay. 1981. Measurement and data analysis. 191-274 in D.M. Gary and D.H. Male (eds.) *Handbook of Snow*, Pergamon Press, 776p.

Gratton, D.J., P.J. Howarth and D.J. Marceau. 1994. An investigation of terrain irradiance in a mountain glacier basin. *Journal of Glaciology* **40**(136): 519-526.

Hannah, D.M. and G.R. McGregor. 1997. Evaluating the impact of climate on snow and ice melt dynamics in the Tai Mon basin, French Pyrénées. *Journal of Glaciology* **43**(145): 563-568.

Hay, J.E. and B.B. Fitzharris. 1988. A comparison of the energy balance and bulk aerodynamic approaches for estimating glacier melt. *Journal of Glaciology* **34**(117): 145-153.

Holmgren, B. 1971. Climate and energy exchange on a sub-polar ice cap in summer. Part C. On the katabatic winds over the northwest slope of the ice cap. Variations of the surface roughness. *Meteorologiska Institutionen Meddelande* **109**, Uppsala Universitet, 43p.

Idso, S.B., and R.D. Jackson. 1969. Thermal radiation from the atmosphere. *Journal of Geophysical Research* **74:** 5397-5403.

Kuhn, M. 1987. Micrometeorological conditions for snow melt. *Journal of Glaciology* **33**(113): 24-26.

Letréguilly, A. 1988. Relation between the mass balance of western Canadian mountain glaciers and meteorological data. *Journal of Glaciology* **34**(116): 11-18.

Lettau, H.H. 1969. Note on aerodynamic roughness parameter estimation on the basis of roughness element description. *Journal of Applied Meteorology* **8:** 828-832.

Lewkowicz, A.G. 1985. Use of an ablatometer to measure short-term ablation of exposed ground ice. *Canadian Journal of Earth Science* **22:** 1767-1773.

Male, D.H. and D.M. Gray. 1981. Snow cover ablation and runoff. 360-436 in Gray, D.M. and D.H. Male (eds.), *Handbook of Snow*, Pergamon Press, 776p.

Meesters, A. and M. van den Broeke. 1997. Response of the longwave radiation over melting snow and ice to atmospheric warming. *Journal of Glaciology* **43**(143): 66-70.

Meier, M.F. 1969. Glaciers and water supply. *Journal American Water Works Association* **61**(1): 8-12.

Meier, M.F., W.V. Tangborn, L.R. Mayo and A. Post. 1971. Combined ice and water balances of Gulkana and Wolverine Glacier, Alaska, and South Cascade Glacier, Washington, 1965 and 1966 hydrologic years. *U.S. Geological Survey Professional Paper* 715-A, 23 pp.

Moore, R.D. 1983. On the use of bulk aerodynamic formulae over melting snow. *Nordic Hydrology* **14:** 193-206.

Müller, F. and C.M. Keeler. 1969. Errors in short-term ablation measurements on melting ice surfaces. *Journal of Glaciology* **8**(52): 91-105.

Munro, D.S. and J.A. Davies. 1977. An experimental study of the glacier boundary layer over melting ice. *Journal of Glaciology* **18**(80): 425-436.

Munro, D.S. and J.A. Davies. 1978. On fitting the log-linear model to wind speed and temperature profiles over a melting glacier. *Boundary Layer Meteorology* **15:** 423-437.

Munro, D.S. and G.J. Young. 1982. An operational net shortwave radiation model for glacier basins. *Water Resources Research* **18**(2): 220-230.

Munro, D.S. 1989. Surface roughness and bulk heat transfer on a glacier: comparison with eddy correlation. *Journal of Glaciology* **35**(121): 343-348.

Munro, D.S. 1990. Comparison of melt energy computations and ablatometer measurements on melting ice and snow. *Arctic and Alpine Research* **22**(2): 153-162.

Munro, D.S. 1991. A surface energy exchange model of glacier melt and net mass balance. *International Journal of Climatology* **11:** 689-700.

Nakawo, M. and G.J. Young. 1981. Field experiments to determine the effect of a debris layer on ablation of glacier ice. *Annals of Glaciology* **2:** 85-91.

Oerlemans, J. 1986. Glaciers as indicators of a carbon dioxide warming. *Nature* **320:** 607-609.

Oerlemans, J. 1988. Simulation of historic glacier fluctuations with a simple climate-glacier model. *Journal of Glaciology* **34**(118): 333-341.

Ohmura, A., P. Kasser and M. Funk. 1992. Climate at the equilibrium line of glaciers. *Journal of Glaciology* **38**(130): 397-411.

Oke, T.R. 1987. *Boundary Layer Climates*. London, Methuen, 435p.

Østrem, G. 1966. Mass balance studies on glaciers in Western Canada, 1965. *Geographical Bulletin* **8:** 81-107.

Østrem, G. 1973. The transient snowline and glacier mass balance in southern British Columbia and Alberta, Canada. *Geografiska Annaler* **55A**(2): 93-106.

Paterson, W.S.B. 1994. *The Physics of Glaciers*. Pergamon Press, 480p.

Pomeroy, J.W. 1991. Transport and sublimation of snow in wind-scoured alpine terrain. *International Association of Scientific Hydrology Publication* **205:** 131-190.

Serreze, M.C. and R.S. Bradley. 1987. Radiation and cloud observations on a high arctic plateau ice cap. *Journal of Glaciology* **33**(114): 162-168.

Stefan, K. 1995. Surface energy exchange at the equilibrium line on the Greenland ice sheet during onset of melt. *Annals of Glaciology* **21:** 13-18.

Stenning, A.J., C.E. Banfield and G.J. Young. 1981. Synoptic controls over katabatic layer characteristics above a melting glacier. *International Journal of Climatology* **1:** 309-324.

IAHS(ICSI)/UNEP/UNESCO. 1996. Glacier Mass Balance Bulletin No. **4**, Haeberli, W., M. Hoelzle and S. Suter (eds.). World Glacier Monitoring Service, Zurich, CH.

IAHS(ICSI)/UNEP/UNESCO. 1999. Glacier Mass Balance Bulletin No. **5**, Haeberli, W., M. Hoelzle and R. Frauenfelder (eds.). World Glacier Monitoring Service, Zurich, CH.

van den Broeke, M.R. 1997a. Structure and diurnal variation of the atmospheric boundary layer over a mid-latitude glacier in summer. *Boundary-Layer Meteorology* **33:** 183-205.

van den Broeke, M.R. 1997b. Momentum, heat and moisture budgets of the katabatic wind layer over a mid-latitude glacier in summer. *Journal of Applied Meteorology* **36**(6): 763-774.

van de Wal, R.S.W., J. Oerlemans and J.C. van der Hage. 1992. A study of ablation variations on the tongue of Hintereisferner, Austrian Alps. *Journal of Glaciology* **38:** 319-324.

Walters, R.A. and M.F. Meier. 1989. Variability of glacier mass balances in western North America. *Geophysical Monographs* **55:** 365-374.

Weller, G.E. 1968. The heat budget and heat transfer processes in Antarctic plateau ice and sea ice. *Australian National Antarctic Research Expeditions Scientific Reports* **102**, 155p.

Wendler, G. 1986. The "radiation paradox" on the slopes of the Antarctic Continent. *Polarforschung* **56**(1/2): 33-41.

Yarnal, B. 1984. Relationship between synoptic weather maps from gridded atmospheric pressure surface data. *Journal of Glaciology* **30**(105): 188-198.

Young, G.J. 1981. The mass balance of Peyto Glacier, Alberta, Canada, 1965-1978. *Arctic and Alpine Research* **13**(3): 307-318.

Paul Cutler came to the University of Toronto in 1989 for post-graduate research in glaciology, after completing his studies at Manchester University, where field work on Gornergletscher had first directed his thoughts toward glaciers. This led to doctoral studies at the University of Minnesota, where Storglaciären was the object of his research. Paul took up his current post-doctoral position at the University of Wisconsin in 1997, where modelling the dynamics of the Laurentide Ice Sheet is presently the focus of his attention. The University of Toronto was Paul's introduction to Peyto Glacier where he worked with Scott Munro on surface reflectivity, subsequently producing the first in his growing list of papers on glaciology. Indications are that, as Paul Cutler continues to publish, this list of publications will reflect his considerable range of field experience studying sub-glacial hydrology and meltwater characteristics of valley glaciers in the Swiss Alps, glacier surface variability of solar radiation absorption in the Canadian Cordillera, sediment loading and discharge characteristics of pro-glacial streams in Pakistan, microclimatic controls on glacier hydraulics in Sweden, Quaternary climate records in Alaskan lake sediment cores, and causes of fast flow in Ice Stream C of West Antarctica. As to his current research focus, few tasks present as great a challenge as that of reconstructing the fluctuations and hydrology of an ice-sheet which no longer exists, but the task is tenable in view of the lessons learned from field work, among them the lessons learned at Peyto Glacier.